THE JOURNAL OF PHYSICAL CHEMISTRY LETTERS
A JOURNAL OF THE AMERICAN CHEMICAL SOCIETY

pubs.acs.org/JPCL

Letter

State Tracking in Nonadiabatic Molecular Dynamics Using Only Forces and Energies

Alexey V. Akimov*

Cite This: J. Phys. Chem. Lett. 2024, 15, 11944−11953

Read Online

ACCESS | Metrics & More | Article Recommendations | Supporting Information

ABSTRACT: A new algorithm for the identification of unavoided (trivial) crossings in nonadiabatic molecular dynamics calculations is reported. The approach does not require knowledge of wave functions or wave function time overlaps and uses only information on state energies and gradients. In addition, a simple phase consistency correction algorithm for time-derivative nonadiabatic couplings is proposed for situations in which wave function time overlaps are not available. The performance of the two algorithms is demonstrated using several state crossing models. The approaches work best for systems with localized nonadiabatic coupling regions but may have difficulties for those with extended regions of nonadiabatic coupling. It is found that state tracking alone is not sufficient for producing correct population dynamics and that nonadiabatic coupling phase correction is required.

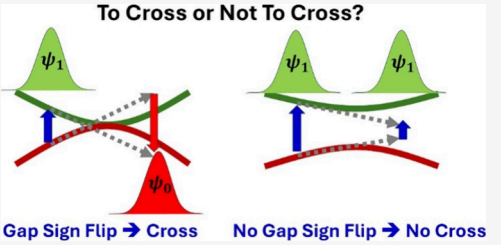

Nonadiabatic molecular dynamics (NA-MD) has become a popular tool for modeling a multitude of photophysical and photochemical processes in biological molecules,[1−6] natural photosynthetic systems,[7−9] and artificial solar energy materials.[10−12] In particular, NA-MD approaches based on the trajectory surface hopping (TSH)[13−16] idea are widely used for modeling charge transfer,[17−20] excitation energy transfer,[7,21] nonradiative electron−hole recombination,[22−24] charge carrier trapping,[25,26] singlet fission,[21,27,28] photoinduced bond breaking or photoisomerization, and many other processes in molecular and solid-state systems[29−31] with up to several thousands of atoms.[32,33]

To date, multiple TSH schemes[15,14,34−38] and their corrections accounting for factors such as electronic decoherence[39−44] or quantum nuclear effects[45−49] have been developed. Although the essential machinery of the TSH methods may be straightforward mathematically, their practical implementation often needs a certain amount of care[50] because at least two kinds of ambiguities in the electronic states are involved. First, the adiabatic states in terms of how many TSH schemes are formulated are determined up to a complex phase factor.[51−53] Second, the identities of the adiabatic states can change along nuclear trajectories.[54−56]

The first problem is the phase inconsistency problem, which originates from the conventions used in the eigensolver algorithms used to construct the adiabatic states and cannot be corrected within the eigensolver algorithm implementation because the latter has information on only a single geometry of the system. The phases should be made consistent with each other in the dynamical algorithms, in which case, information about more than one geometry is used. Missing the phase corrections was shown to lead to incorrect population dynamics.[51]

The second problem concerns the possibility of state crossings, which may change state identities along their trajectories. Tracking states is critically important in these situations, because missing it can result in an incorrect assignment of state populations[57] and introduce artifacts such as unphysical long-range charge transfer effects.[55,58] While the adiabatic states are typically ordered according to their energies, this ordering may be different from the ordering based on the character of states (their identity). The most prominent situation causing such state crossing is if the corresponding diabatic states have zero diabatic coupling, and the energies of the corresponding diabats cross. The crossing may be caused by a small geometric perturbation if the system already resides near the state crossing point in the phase space. In this situation, if the system is treated as residing on the starting adiabatic state, the corresponding nuclear forces would be discontinuous, leading to problems in evolving nuclear dynamics even adiabatically (although in this situation, using the adiabatic dynamics would be incorrect in the first place).

Not changing the adiabatic state index in an appropriate way may lead to other artifacts. For instance, electronic states localized on well-separated molecules in a molecular crystal would be non-interacting, yet their energies may change in an uncorrelated way due to small geometric perturbations, causing frequent crossings of the corresponding adiabatic states. This

Received: October 7, 2024
Revised: November 6, 2024
Accepted: November 20, 2024
Published: November 22, 2024

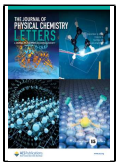

situation is known as trivial or "unavoided" crossing. Following the adiabatic state with the unchanged state index would result in a spurious charge transfer from one end of the molecular crystal to the other. As a result, following the incorrect state index could lead to unphysical long-range charge transfer and yield overestimated and nonconverging charge carrier mobilities.

Yet another example of trivial crossing would be the crossing of electronic states of different spin multiplicities. If no spin−orbit coupling is included or present (or if it is negligible), singlet and triplet states (for instance) can cross without interacting with each other. Staying in the adiabatic state corresponding to the lowest energy would erroneously result in a spin-forbidden electronic transition. Thus, tracking state identities and detecting the trivial crossings are greatly important for a meaningful interpretation of the excited-state dynamics results.

To date, several state-tracking algorithms have been developed,[54,59−61] but all of them rely on the use of wave function ($\{\psi_i\}$) time overlaps, $S_{ij}(t, t+\Delta t) = \langle \psi_i(t)|\psi_j(t+\Delta t)\rangle$ (hence they are hereafter termed S tracking), which may be difficult if not prohibitive to compute for sophisticated electronic structure methods, even if the wave functions are available. For instance, multiconfigurational excited-state wave functions are represented as superpositions of a large number of N-electron Slater determinants, $\Phi_I = \frac{1}{\sqrt{N!}}|\psi_{i_1}\psi_{i_2}...\psi_{i_N}|$. The computation of the excited-state time overlaps then involves calculations of the time overlaps for many pairs of Slater determinants. While computing the time-derivative nonadiabatic couplings (tNACs) of Slater determinants, $\langle \Phi_I|\frac{\partial}{\partial t}|\Phi_J\rangle$, can be reduced to tNAC calculations for suitable single-particle orbitals,[60,62] $\langle \psi_I|\frac{\partial}{\partial t}|\psi_j\rangle$, no such simplification for the time overlaps was reported. For solid-state systems, the correlated wave functions obtained from the many-body GW or Bethe−Salpeter equation (BSE) involve summations over millions if not billions of products of electron and hole orbitals and over multiple combinations of wavevectors.[30,63−65] Thus, the computation of the GW or BSE wave function time overlaps is a computationally challenging task, which may be comparable in cost to if not more costly than solving for such wave functions themselves. As a consequence, time overlap calculations are still out of reach for many advanced electronic structure calculations, making it impractical to use the existing time overlap-based state-tracking approaches in such calculations.

On the contrary, state-resolved gradients and energies are available for many electronic structure methods ranging from commonly used time-dependent density functional theory (TD-DFT)[66,67] approaches to much more sophisticated methods such as state-specific complete active-state pair density functional theory (SS-CAS-PDFT).[68] Thus, it is natural to look for trivial crossing identification algorithms that would rely on the use of only state energies and gradients. In line with this philosophy, recent NA-MD developments incentivized the use of only energies, gradients, and energy curvatures (NAC-free NA-MD method)[69−74] as an alternative to the traditional reliance on NACs when solving the time-dependent Schrodinger equation (TD-SE) and conducting TSH calculations. Therefore, having the state-tracking algorithm that requires wave function time overlaps would be an inconvenient redundancy for NAC-free NA-MD methods. In other scenarios, one may still want to use NACs when integrating the TD-SE but may not have sufficient additional information such as the wave function time overlaps needed to properly track states and account for NAC phases.

In this work, I report simple algorithms for (a) the identification of trivial crossings that relies on only easily accessible information such as state gradients and energies rather than on much more tedious-to-compute wave function time overlaps and (b) the correction of phases of time-derivative NAC (tNAC) matrix elements used in the TD-SE integration and TSH schemes. These algorithms are designed primarily for situations in which time overlaps are not accessible. Hence, although the current proof of principle is demonstrated with the model problems, a particular strength of the methodology would be for atomistic simulations with many-body electronic structure methodologies, although such calculations are outside of the scope of this work.

The generic NA-MD algorithm has been described many times in various sources.[34,41,75] Here, I only briefly overview the basic definitions and equations. First, the electron−nuclear wave function is described by the simplified Born−Huang ansatz:

$$\Psi(t, \mathbf{r}; \mathbf{q}) = \sum_i c_i(t)\psi_i(\mathbf{r}; \mathbf{q}(t)) \tag{1}$$

where $\{\psi_i[\mathbf{r}; \mathbf{q}(t)]\}$ is the basis of electronic adiabatic wave functions, which are parametrically dependent on nuclear trajectories $\mathbf{q}(t)$. Here, $\{c_i(t)\}$ is the corresponding amplitude of the adiabatic states. Throughout this work, bold symbols refer to vectors and matrices. The dynamics of nuclei is described by classical Newtonian equations of motion:

$$\dot{\mathbf{q}} = \mathbf{M}^{-1}\mathbf{p} \tag{2a}$$

$$\dot{\mathbf{p}} = \mathbf{F} \tag{2b}$$

where $\mathbf{M} = \mathrm{diag}(m_0, m_1, ..., m_{N_{\mathrm{dof}}-1})$ is the diagonal matrix of masses of N_{dof} nuclear degrees of freedom, $\mathbf{p}$ is the vector of nuclear momenta, and $\mathbf{F}_a$ is the vector of nuclear forces corresponding to active adiabatic state a.

The electronic dynamics is described by the TD-SE, which in the adiabatic basis takes the form

$$i\hbar\frac{\partial c_i(t)}{\partial t} = \sum_j H_{ij}^{\mathrm{vib}}(t)c_j(t) \tag{3}$$

where $H_{ij} = E_i\delta_{ij} - i\hbar d_{ij}$ is the vibronic Hamiltonian matrix element, E_i is the adiabatic energy of state i, δ_{ij} is the Kronecker delta, and $d_{ij} = \langle \psi_i|\frac{\partial}{\partial t}|\psi_j\rangle = \mathbf{h}_{ij}^T\mathbf{M}^{-1}\mathbf{p}$ is the scalar time-derivative nonadiabatic coupling, tNAC, also known as scalar NACs. Finally, $\mathbf{h}_{ij} = \langle \psi_i|\nabla_{\mathbf{q}}|\psi_j\rangle$ is the nonadiabatic coupling vector, abbreviated simply as NAC. The NAC abbreviation is also used in general context, when it is not important whether one thinks of the scalar or vectorial property. The evolved amplitudes are used to compute state hopping probabilities using the global flux surface hopping (GFSH) prescription of Wang et al.[76] and the Jasper−Truhlar criteria[77] for velocity reversal criteria at the frustrated hops. Together with the newly introduced state-tracking and NAC phase correction algorithms, the following alternatives are used: a generalized local diabatization (LD)-based approach[78] similar to that of Granucci and co-workers,[79] the min-cost algorithm of Fernandez-Alberti and co-workers,[59] and the phase correction I previously reported.[51] Further details and discussion of the basic methodologies are summarized in section S1 of the Supporting Information, while the rest of the work will focus on the new approach.

https://doi.org/10.1021/acs.jpclett.4c02909
J. Phys. Chem. Lett. 2024, 15, 11944−11953

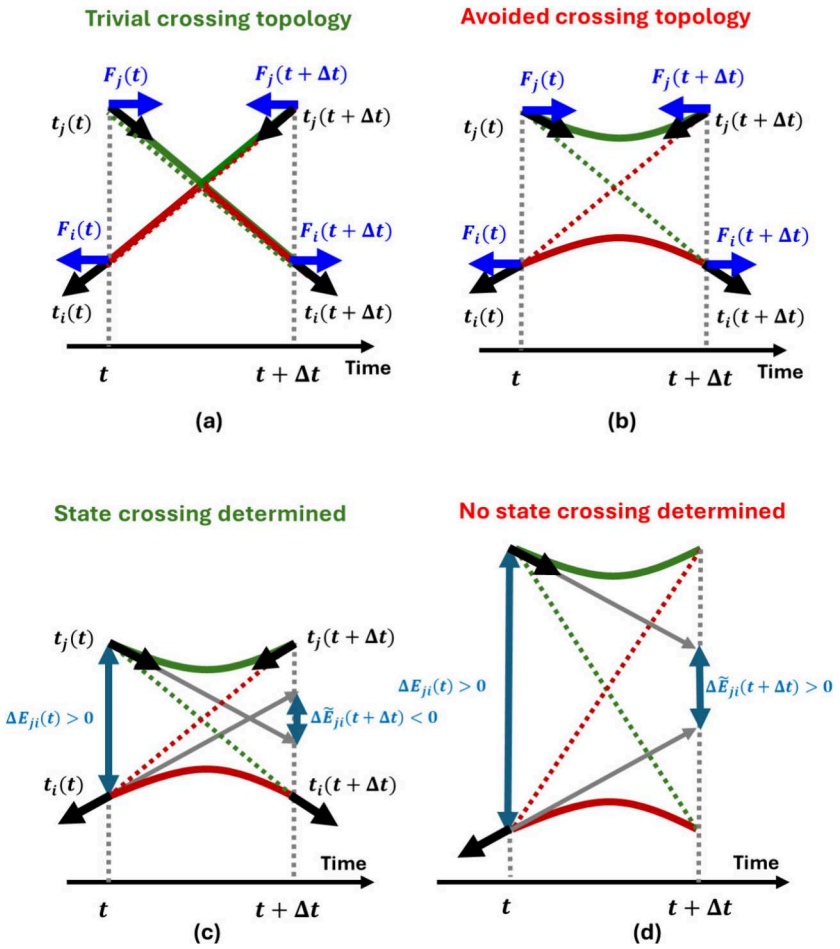

Figure 1. Conceptual idea of the F-tracking algorithm. (a) Trivial crossing topology, directions of the tangents, t_i, and corresponding force components, F_i. (b) Tangents/force signature similar to those of the trivial crossing topology can occur in the avoided crossing topology; this example demonstrates that using only force signs is not sufficient to detect trivial crossings. (c) Close-up of a small gap topology near the state crossing. The extrapolated energy gap, $\Delta\tilde{E}_{ji}$, changes the sign; the trivial state crossing is determined. (d) Larger gap situation with the same forces in which when no change in the sign of the extrapolated energy gap is determined, no state crossing occurs. The solid green and red lines indicate the adiabatic-state energy profiles, while the dashed lines indicate the corresponding diabatic curves. Gray arrows indicate the change of the state energies while moving on these surfaces for time Δt under the motion of the corresponding state forces.

The proposed F-tracking approach is rooted in the principle of property continuity. As mentioned in the introduction, following the incorrect state index in the adiabatic dynamics may lead to discontinuities of state forces and violate the energy conservation requirement. Thus, at a trivial state crossing or an avoided crossing with a sufficiently small adiabatic gap, the active state should be chosen such that the change in force is minimal when the system crosses the intersection point. This approach enforces the continuity of state forces along the system's trajectory. The S-tracking algorithm follows the same general principle, enforcing the maximum continuity, is but applied to wave functions. In this approach, I assume the information on wave functions is inaccessible but the information on the derived properties such as state gradients is. In this approach, the forces act as descriptors specific to the nature of the state.

To better understand the force continuity enforcement as a principle for state tracking, consider the two-state crossing model depicted in Figure 1. In Figure 1a, the crossing of non-interacting diabatic surfaces (dashed lines) yields the trivial crossing topology of the adiabatic potential energy surfaces. In this case, following the initial diabat (but switching to a different adiabat) is expected, because the diabatic coupling is zero and no transition between diabatic states is possible. In this scenario, the forces for the active state are minimally perturbed, and no force discontinuity problem arises. For example, state j at time t should change to state i at time $t + \Delta t$, because the corresponding forces $\mathbf{F}_j(t)$ and $\mathbf{F}_i(t + \Delta t)$ would maintain their direction, while continuing on the same state j would lead to a change in the sign of the adiabatic force, $\mathbf{F}_i^T(t)\mathbf{F}_j(t + \Delta t) < 0$. However, considering only the changes of force directions is not sufficient for a correct assignment of states. Indeed, the same force signature as in Figure 1a is also encountered in the case of interacting diabatic surfaces, leading to the avoided crossing topology of the intersection (Figure 1b). At the same time, the adiabatic gap in this situation may be quite large and no state index change should occur.

To factor the energy change component into the state-tracking algorithm, consider a fictitious evolution of the system on both involved surfaces under the action of the corresponding state-specific forces at the beginning of the time step (Figure 1c). On the basis of the definition of the force component along direction α, $F_{i,\alpha} = -\frac{\partial E_i}{\partial R_\alpha}$, one can expect that during time step Δt, the energy of state i changes by

https://doi.org/10.1021/acs.jpclett.4c02909
J. Phys. Chem. Lett. 2024, 15, 11944−11953

$$\Delta E_i(t+\Delta t) = -\sum_\alpha F_{i,\alpha}(t)\Delta R_\alpha = -\sum_\alpha F_{i,\alpha}(t)\left[M_\alpha{}^{-1}P_\alpha\left(t+\frac{\Delta t}{2}\right)\Delta t + \frac{1}{2}M_\alpha{}^{-1}F_{i,\alpha}(t)\Delta t^2\right] \quad (4)$$

where P_α is the nuclear momentum and M_α is the mass of nuclear degree of freedom α. Analogous changes can be computed for energy E_j. The extrapolated energy gap will be

$$\Delta\tilde{E}_{ji}(t+\Delta t) = \Delta E_{ji}(t) + \Delta E_j - \Delta E_i = \Delta E_{ji}(t) - \sum_\alpha [F_{j,\alpha}(t) - F_{i,\alpha}(t)]M_\alpha{}^{-1}P_\alpha\left(t+\frac{\Delta t}{2}\right)\Delta t - \frac{1}{2}\sum_\alpha [F_{j,\alpha}{}^2(t) - F_{i,\alpha}{}^2(t)]M_\alpha{}^{-1}\Delta t^2 \quad (5)$$

This extrapolated gap reflects the change in the adiabatic energy gap upon the nuclear displacements, $\Delta R_\alpha = M_\alpha{}^{-1}P_\alpha\Delta t + \frac{1}{2}M_\alpha{}^{-1}F_\alpha\Delta t^2$ under the action of initial forces and momenta for a duration of Δt. The sign reversal of the extrapolated gap compared to the initial energy gap is more likely to occur when surfaces have a sharper crossing topology, like in Figure 1a. Figure 1c shows a close-up of a similar situation of a finite but still relatively small energy gap for which a change in state identity is likely to occur (a near-trivial-crossing situation). As the energy gap increases (Figure 1d), the sign reversal of the extrapolated energy gap is less likely to occur, suggesting that no state identity change occurs, as expected for adiabatic regimes.

In practice, the state permutations are found by applying the Munkres–Kuhn (min-cost) algorithm[59] to cost matrix **C** with the matrix elements defined as

$$C_{ij} = \left|\frac{1}{2}\{1 - \mathrm{sign}[\Delta E_{ji}(t)]\mathrm{sign}[\Delta\tilde{E}_{ji}(t+\Delta t)]\}\right|^2 \quad (6)$$

This formula yields larger costs (of 1) for the pairs of states that exhibit trivial crossing (flip of the sign of the extrapolated energy gap compared to the starting one) and the smallest values (0) when the states do not cross. For the diagonal elements of the matrix, one obtains intermediate values of $(1/2)^2 = 0.25$, which is overwhelmed by the off-diagonal elements of 1.0, when trivial crossings occur. The choice of the cost matrix is not unique, and it is currently chosen as a simple yet physically motivated one.

For the S- and F-tracking approaches, the obtained state permutation matrix is used to transform the state amplitude vectors in the TD-SE integration procedure. It is also applied to permute state indices. In the generalized LD approach, a continuous analogue of such a "permutation" matrix is constructed as described elsewhere.[78,80] It is used to directly transform the state amplitude vectors and determine the reordering of the adiabatic-state indices. Additional details are given in section S1.

The proposed approach is an ad hoc method based on physical intuition and the principle of force continuity. It is not guaranteed to work flawlessly in all situations, but it could be the only viable solution in some situations. As mentioned in the introduction, one of these situations is that in which wave functions or time overlaps are not available or too costly to compute, while state energies and gradients are accessible. For instance, for methods such as GW, storing the wave function for just a single state may take gigabytes of memory, due to summation over k-points and distinct single-particle excitations. The computation of the time overlaps may become comparable in cost to if not more computationally intensive than obtaining the wave functions themselves. In addition, the use of the wave function overlap is conceptually flawed for perturbation-based methods. While such methods can yield accurate state energies and gradients, the corresponding wave functions are not self-consistent and hence may lack orthonormality, hence requiring generalization of the corresponding NAD formalism to non-orthogonal states.

On the basis of the construction, the approach is expected to work best in situations of clear trivial crossings (zero diabatic couplings) of isolated pairs of states. As the diabatic coupling increases, the adiabatic-state energy profiles may become more distant from the corresponding diabats, especially when many diabatic states are strongly mixed. In this situation or larger adiabatic gaps, the presented algorithm for state mapping may become confused. For the avoided crossing situations (when the diabatic coupling is non-zero), the algorithm is expected to follow the adiabatic surface (without state reordering) even if they are separated by a very small energy gap. Indeed, with the small integration time step parameter, Δt, one may be nearly at the potential energy surface minimum where forces nearly vanish. At this position, the change in the energy gap is negligible, and the gap conserves its sign, leading to the cost matrix elements being zero. This situation means that no state index swap would occur and the state identities would be preserved. However, a small diabatic coupling makes the adiabatic surfaces resemble more the corresponding diabatic characters. In this regard, the closely spaced adiabatic states may change their character when passing the avoided crossing point, and state switching may be detected. In more complex situations of multiple diabatic-state crossings, when some diabatic couplings are small and others are large, the gap between a pair of adiabatic states may bracket multiple crossing diabatic curves. In this situation, the F-tracking approach may miss the detection of the correct pair of indices corresponding to the crossing states. Further improvements in the cost matrix element (eq 6) may be able to account for such situations, but this topic is outside the scope of this work.

In addition to the presented state-tracking algorithm, I present a new approach to ensure the phase consistency of tNACs. In practical calculations, especially for extended atomistic systems, tNACs may be available when the time overlaps are not. In this situation, the phase correction to tNACs[51] cannot be computed using standard approaches. Indeed, while the tNACs can often be computed from the wave function time overlaps,[81] they can also be obtained in NAC-free ways[70] or analytically. Thus, it is desirable to rely solely on such information without resorting to time overlaps.

The phase correction presented here is based on another observation. Considering that trivial crossing is often localized in space and typically involves only two states, one can assume that the tNACs should be continuous and behave as a Lorentzian function of the effective one-dimensional (1D) reaction coordinate.[71] For 1D model Hamiltonians such as those considered in this work, such a coordinate choice is natural. In atomistic simulations with multidimensional Hamiltonians, this reaction coordinate can coincide with the nuclear trajectory. Alternatively, one can think of the projection of the NAC vector on the nuclear velocity direction. Due to the Lorentzian

https://doi.org/10.1021/acs.jpclett.4c02909
J. Phys. Chem. Lett. 2024, 15, 11944−11953

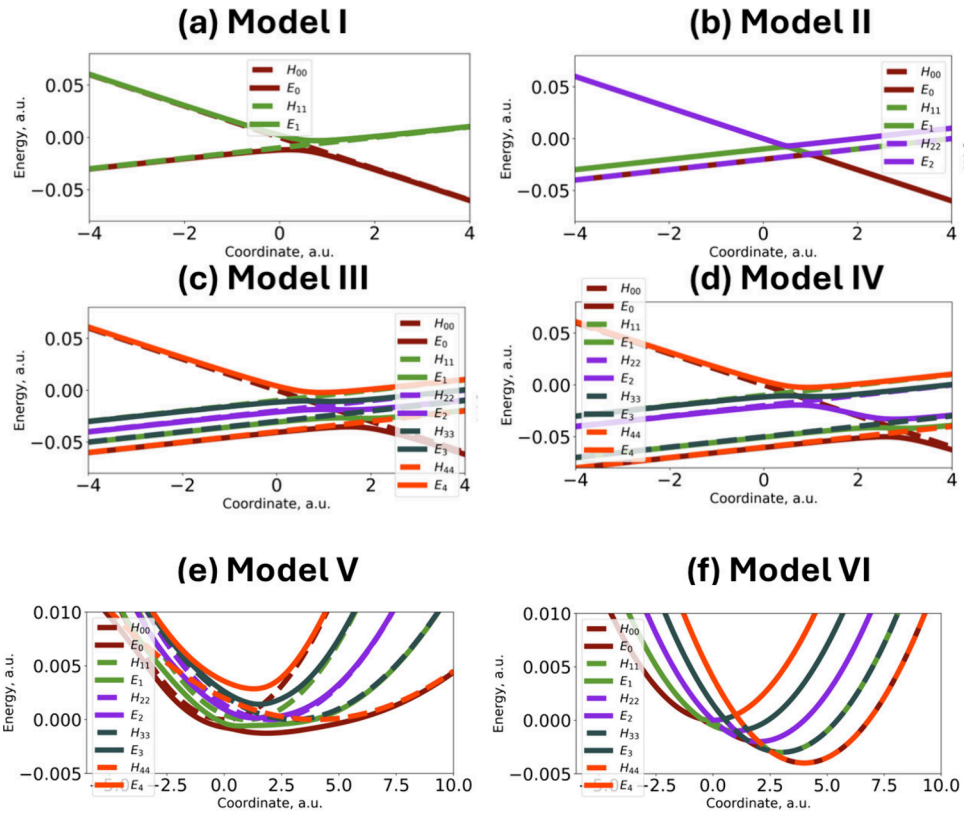

Figure 2. Adiabatic and diabatic energy profiles for the six models used in this work. Solid lines represent adiabatic energy levels, while the dashed lines the diabatic ones.

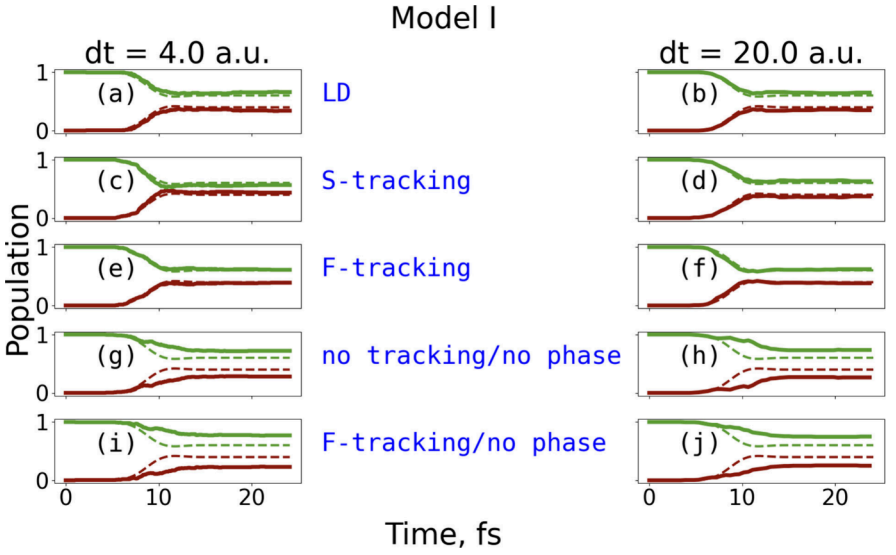

Figure 3. Results of NA-MD calculations for model I obtained using integration time steps of (a, c, e, g, and i) 4 au and (b, d, f, h, and j) 20 au and different state-tracking and phase correction algorithms. Solid lines represent the TSH results, and dashed lines the SOFT results. Adiabatic-state color codes: red for 0 and green for 1.

functional form, the NAC for a given pair of states shall not change its sign during the passage of the state crossing, although the NACs for different pairs of states may have different signs. Naturally, the antisymmetry of tNACs, $d_{ij} = -d_{j,i}$, should also be maintained. As a result, the tNAC phase correction takes the following form:

$$s_{ij} = \mathrm{sign}[d_{ij}(t - \Delta t)]\mathrm{sign}[d_{ij}(t)],\ i > j \tag{7a}$$

$$d_{ij}(t) \rightarrow \tilde{d}_{ij}(t) = d_{ij}(t)s_{ij} \tag{7b}$$

$$d_{ji}(t) \rightarrow \tilde{d}_{ji}(t) = d_{ji}(t)s_{ij} \tag{7c}$$

As mentioned above, the assumption that tNAC behaves as a continuous function is justified only in the case of localized (weak diabatic coupling) two-state crossings. In a situation of stronger diabatic couplings or nonconstant diabatic coupling,

https://doi.org/10.1021/acs.jpclett.4c02909
J. Phys. Chem. Lett. 2024, 15, 11944−11953

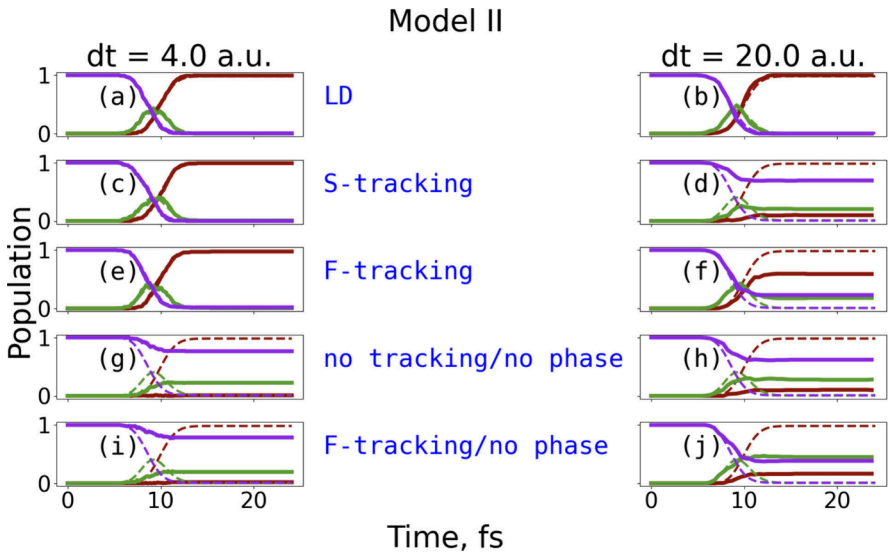

Figure 4. Results of NA-MD calculations for model II obtained using integration time steps of (a, c, e, g, and i) 4 au and (b, d, f, h, and j) 20 au and different state-tracking and phase correction algorithms. Solid lines represent TSH results, and dashed lines SOFT results. Adiabatic-state color codes: red for 0, green for 1, and purple for 2.

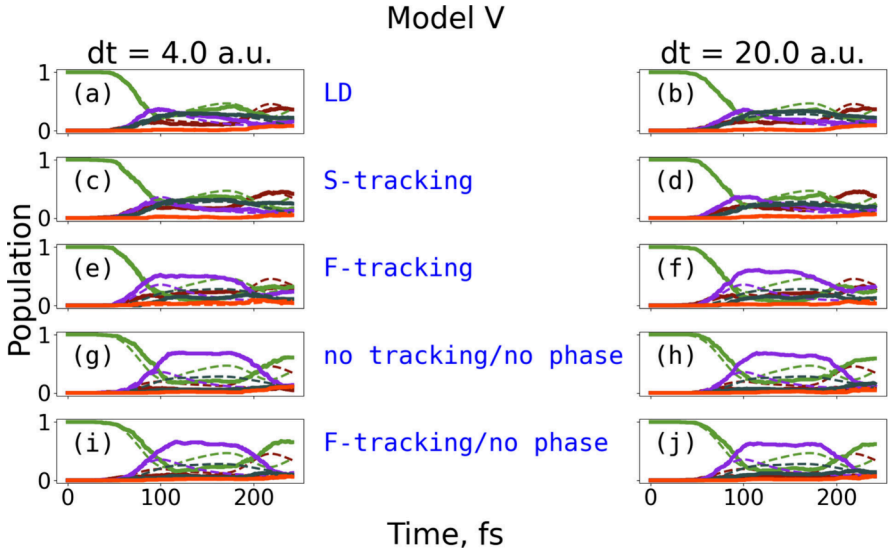

Figure 5. Results of NA-MD calculations for model II obtained using integration time steps of (a, c, e, g, and i) 4 au and (b, d, f, h, and j) 20 au and different state-tracking and phase correction algorithms. Solid lines represent TSH results, and dashed lines SOFT results. Adiabatic-state color codes: red for 0, green for 1, purple for 2, dark cyan for 3, and orange for 4.

the width of the NA coupling region may be substantial. In addition, one may construct models in which multiple states actively interact. In both of these cases, a continuous evolution of the tNAC matrix elements may naturally lead to their sign reversal. In this situation, this simple phase correction (eq 7) is likely to break down.

The new state-tracking and phase correction algorithms are tested using eight model Hamiltonians (Figure 2). The first four models (I–IV, Figure 2, panels a–d, respectively) are the linear crossing models of Esch and Levine[82] also utilized in recent methodology development[75] and assessment[41] studies. Models V and VI (Figure 2, panels e and f, respectively) are given by the Holstein-type Hamiltonians, similar to those employed in other studies.[47,75,78] Finally, models VII and VIII are the three-state, three-nuclear DOF spin-boson Hamiltonian of Wang and Prezhdo[58] and the five-state, five-nuclear DOF spin-boson Hamiltonian of Jain, Alguire, and Subotnik,[43] respectively. The detailed definition of the models is given in section S2.

All TSH methods and model Hamiltonian construction functions are implemented in Libra.[83,84] The methods reported here are included in the new release of the Libra code, version 5.8.1,[85] prepared together with this work. The details of TSH and quantum simulations are presented in section S3. In addition, the scripts for conducting all presented calculations are available in the public Zenodo repository.[86]

Here, I compare the performance of the five tracking/phase correction approaches (Figures 3–6 and Figures S1–S4 for models I–VIII): (i) generalized local diabatization (LD) approach[78] (panels a and b) similar to that of Granucci and co-workers,[79] (ii) S tracking based on the min-cost algorithm combined with the phase correction of tNACs,[51] in which the TD-SE is integrated using tNACs (panels c and d), (iii) present F-based tracking scheme combined with the present tNAC

https://doi.org/10.1021/acs.jpclett.4c02909
J. Phys. Chem. Lett. 2024, 15, 11944–11953

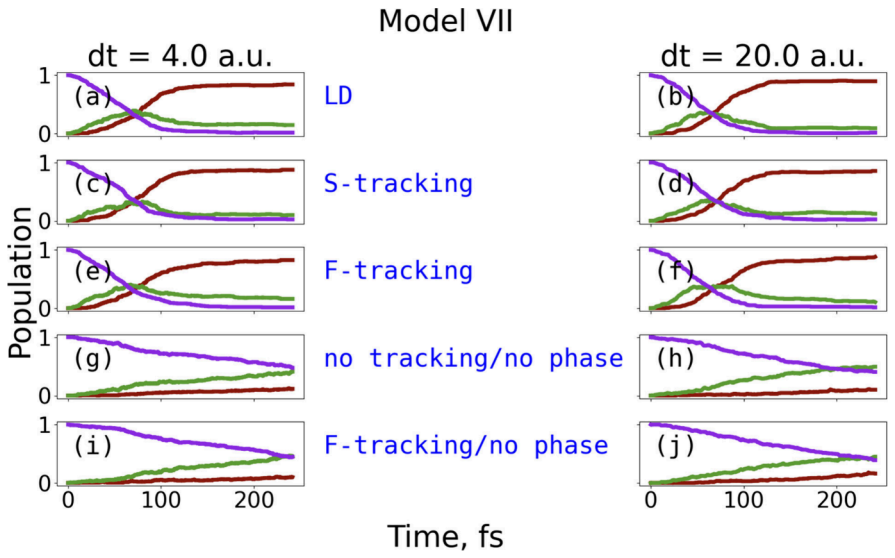

Figure 6. Results of NA-MD calculations for model VII obtained using integration time steps of (a, c, e, g, and i) 4 au and (b, d, f, h, and j) 20 au and different state-tracking and phase correction algorithms. Adiabatic-state color codes: red for 0, green for 1, and purple for 2.

phase correction approach (eq 7) (panels e and f), (iv) the application of neither state tracking nor phase corrections (panels g and h), and (v) the same approach as approach iii but without tNAC phase correction (panels i and j). In addition, the results from the fully quantum calculations are shown in the dashed lines for 1D problems I−VI. For multidimensional models VII and VIII, we primarily aim to compare the performance of the new F-tracking/tNAC phase correction approaches to that of the LD approach, considered a second reference (after the fully quantum calculations).

I first discuss the results for models I−IV. Using a relatively small integration time step of 4.0 au (left column of Figures 3 and 4 and Figures S1 and S2), all approaches but iv and v yield good agreement with the fully quantum results. Naïve approach iv without tracking and phase corrections always fails to yield correct dynamics. However, state tracking alone (method v) still cannot yield the correct dynamics, in most cases. Thus, the phase correction is critical to include together with the state-tracking algorithm.

Among the LD and S- and F-tracking approaches, the LD approach is the most robust; for models I−IV, it always yields nearly a quantitative agreement with the SOFT reference, even for the larger integration time step. Both S and F tracking (together with the new tNAC phase correction) yield accurate dynamics for all four models and both integration time steps used, with the only exception being model II and a larger Δt of 20 au, in which case both S- and F-tracking approaches break down (Figure 4). The breakdown of the S-tracking approach can be attributed to numerical inaccuracies of the TD-SE integration because large tNACs are still involved. The breakdown of the F-tracking approach inherits this reason. In addition, F tracking requires sufficiently small integration time steps for accurate extrapolation of the energy gap change.

Surprisingly, for models I (Figure 3), III (Figure S1), and IV (Figure S2), the F-tracking scheme shows slightly better agreement with the SOFT-derived populations than even the commonly adopted S-tracking approach, although this observation is not necessarily systematic.

While the encouraging results for models I−IV confirm the utility of the F-tracking and new phase correction approaches, the calculations for model V (Figure 5) suggest that the F-tracking approach may break down in situations with a broader region of nonadiabatic coupling. As I have already shown in Figure 2e, the adiabatic gaps between some states may enclose multiple diabats rather than being closely related to only two "parent" diabats as in all examples considered so far (models I−IV). As a result, the algorithm may not be able to recognize and "choose" the correct diabat along which the system would travel in the diabatic representation. As a consequence, the selection of the state may be incorrect, leading to observed deviations of the evolved populations from the SOFT-derived references. When this limitation of the F-tracking approach is considered, not using any state tracking or not including phase correction of tNACs leads to even stronger deviations of the computed populations from the reference values. In this sense, having both F tracking and the simplistic tNAC phase correction does help improve the dynamics, but such an approach still remains inferior to LD and S tracking.

To test the attribution of the failure of the F-tracking approach for model V to the degree of tNAC locality described above, consider model VI that features multiple trivial crossings with highly localized nonadiabatic regions (Figure 2f). The TSH calculations demonstrate that F tracking yields dynamics consistent with that obtained by other methods such as LD, S tracking, and reference SOFT calculations (Figure S3a−f). Moreover, the tNAC phase correction is not critical for this model (Figure S3i,j). At the same time, not having any state tracking yields vastly incorrect dynamics (Figure S3g,h). This model demonstrated that accounting for only sign changes of tNAC is not sufficient to produce the correct dynamics and that the state-tracking component is essential.

Finally, to demonstrate the utility of the new approaches for multidimensional problems, I study the dynamics in two spin-boson systems: a three-state, three-nuclear DOF model VII (Figure 6) and a five-state, five-nuclear DOF model VIII (Figure S4). While exact population dynamics for such cases is not computed, the quality of the F-tracking and tNAC phase correction approaches can be judged on the basis of a comparison to the dynamics obtained with the LD approach. For model VII, the F-tracking approach yields dynamics similar to those obtained with both LD and S tracking (Figure 6a−f). This result holds for both small and larger integration time steps.

https://doi.org/10.1021/acs.jpclett.4c02909
J. Phys. Chem. Lett. 2024, 15, 11944−11953

Omitting tNAC phase correction and state tracking (panels g and h) or even the tNAC correction alone (panels i and j) results in qualitatively different dynamics. For more complex model VIII (Figure S4), both S- and F-tracking approaches yield similar results for the smaller integration time step but show notably different population dynamics as the integration time step is increased. The more accurate calculations with the small time steps are still notably different from the reference LD result, suggesting that even smaller integration time steps may be needed. At the same time, for a larger time step Δt of 20 au, the F-tracking approach yields qualitatively better-behaving population dynamics than the S-tracking approach, as judged by comparing it to that in the LD simulations. Finally, model VIII is yet another example showing the effect of phase correction and state tracking separately; in this case, the computed population dynamics is quite distinct depending on whether the tNAC phase correction is included (Figure S4g–j). However, because no state tracking is used in these cases, the population dynamics is notably distinct from the reference LD-based dynamics, as well as from the S- and F-tracking results.

In summary, a new wave function-, time overlap-, and tNAC-free state-tracking algorithm, dubbed F tracking, is developed and validated using several multistate, 1D and multidimensional model problems that emphasize trivial crossing situations. In addition, a simple wave function- or time overlap-free tNAC phase correction approach is developed. While the F-tracking algorithm itself does not need tNACs or time overlaps, the proposed tNAC phase correction does require information about scalar NACs but does not require knowledge of the time overlap matrices, which are often more difficult to obtain than the scalar tNACs themselves, especially in certain kinds of atomistic calculations. The combination of the F-tracking and simple phase correction approaches is demonstrated to yield good agreement with the S-tracking and LD-based approaches, which all require knowledge of the time overlaps of the states. In some situations, the results of F tracking are even more accurate than those of broadly used S tracking. I demonstrate that state tracking alone often fails to yield correct population dynamics, and using the tNAC phase correction is critical. The new approaches are demonstrated to work best in problems with well-localized tNAC regions (smaller diabatic couplings), where trivial crossings are dominant. They offer simplicity that can be beneficial in model and atomistic situations, especially when time overlaps are not easily accessible. The methods may, however, break down for problems with wide regions of nonadiabatic coupling where multiple diabatic states interact with each other with a variety of diabatic coupling strengths.

■ ASSOCIATED CONTENT

Data Availability Statement

Detailed scripts and input files used for all types of calculations are available in digital form at Zenodo.[86]

Supporting Information

The Supporting Information is available free of charge at https://pubs.acs.org/doi/10.1021/acs.jpclett.4c02909.

Methodological details, definitions of model Hamiltonians, computational details, and simulation results for models not shown in the text (PDF)

Transparent Peer Review report available (PDF)

■ AUTHOR INFORMATION

Corresponding Author

Alexey V. Akimov − *Department of Chemistry, University at Buffalo, The State University of New York, Buffalo, New York 14260, United States;* orcid.org/0000-0002-7815-3731; Email: alexeyak@buffalo.edu

Complete contact information is available at: https://pubs.acs.org/10.1021/acs.jpclett.4c02909

Notes

The author declares no competing financial interest.

■ ACKNOWLEDGMENTS

The author acknowledges financial support from the National Science Foundation (Grant NSF-2045204). Support of computations was provided by the Center for Computational Research at the University at Buffalo.

■ REFERENCES

(1) Zobel, J. P.; Heindl, M.; Plasser, F.; Mai, S.; González, L. Surface Hopping Dynamics on Vibronic Coupling Models. *Acc. Chem. Res.* **2021**, *54* (20), 3760−3771.

(2) Mukherjee, S.; Pinheiro, M.; Demoulin, B.; Barbatti, M. Simulations of Molecular Photodynamics in Long Timescales. *Philos. Trans. R. Soc. Math. Phys. Eng. Sci.* **2022**, *380* (2223), No. 20200382.

(3) Abiola, T. T.; Rodrigues, N. D. N.; Ho, C.; Coxon, D. J. L.; Horbury, M. D.; Toldo, J. M.; Do Casal, M. T.; Rioux, B.; Peyrot, C.; Mention, M. M.; Balaguer, P.; Barbatti, M.; Allais, F.; Stavros, V. G. New Generation UV-A Filters: Understanding Their Photodynamics on a Human Skin Mimic. *J. Phys. Chem. Lett.* **2021**, *12* (1), 337−344.

(4) Toldo, J. M.; Do Casal, M. T.; Barbatti, M. Mechanistic Aspects of the Photophysics of UVA Filters Based on Meldrum Derivatives. *J. Phys. Chem. A* **2021**, *125* (25), 5499−5508.

(5) Barbatti, M.; Aquino, A. J. A.; Szymczak, J. J.; Nachtigallová, D.; Hobza, P.; Lischka, H. Relaxation Mechanisms of UV-Photoexcited DNA and RNA Nucleobases. *Proc. Natl. Acad. Sci. U. S. A.* **2010**, *107* (50), 21453−21458.

(6) Barbatti, M.; Ruckenbauer, M.; Szymczak, J. J.; Aquino, A. J. A.; Lischka, H. Nonadiabatic Excited-State Dynamics of Polar π-Systems and Related Model Compounds of Biological Relevance. *Phys. Chem. Chem. Phys.* **2008**, *10* (4), 482−494.

(7) Ullah, A.; Dral, P. O. Predicting the Future of Excitation Energy Transfer in Light-Harvesting Complex with Artificial Intelligence-Based Quantum Dynamics. *Nat. Commun.* **2022**, *13* (1), 1930.

(8) Cotton, S. J.; Miller, W. H. The Symmetrical Quasi-Classical Model for Electronically Non-Adiabatic Processes Applied to Energy Transfer Dynamics in Site-Exciton Models of Light-Harvesting Complexes. *J. Chem. Theory Comput.* **2016**, *12* (3), 983−991.

(9) König, C.; Neugebauer, J. Protein Effects on the Optical Spectrum of the Fenna−Matthews−Olson Complex from Fully Quantum Chemical Calculations. *J. Chem. Theory Comput.* **2013**, *9* (3), 1808−1820.

(10) C. A. Valente, D.; Do Casal, M. T.; Barbatti, M.; Niehaus, T. A.; Aquino, A. J. A.; Lischka, H.; Cardozo, T. M. Excitonic and Charge Transfer Interactions in Tetracene Stacked and T-Shaped Dimers. *J. Chem. Phys.* **2021**, *154* (4), No. 044306.

(11) Hu, Z.; Sun, X. All-Atom Nonadiabatic Semiclassical Mapping Dynamics for Photoinduced Charge Transfer of Organic Photovoltaic Molecules in Explicit Solvents. *J. Chem. Theory Comput.* **2022**, *18* (10), 5819−5836.

(12) Tinnin, J.; Bhandari, S.; Zhang, P.; Geva, E.; Dunietz, B. D.; Sun, X.; Cheung, M. S. Correlating Interfacial Charge Transfer Rates with Interfacial Molecular Structure in the Tetraphenyldibenzoperiflanthene/C 70 Organic Photovoltaic System. *J. Phys. Chem. Lett.* **2022**, *13* (3), 763−769.

(13) Tully, J. C. Molecular Dynamics with Electronic Transitions. *J. Chem. Phys.* **1990**, *93* (2), 1061−1071.
(14) Barbatti, M. Nonadiabatic Dynamics with Trajectory Surface Hopping Method. *WIREs Comput. Mol. Sci.* **2011**, *1* (4), 620−633.
(15) Wang, L.; Akimov, A.; Prezhdo, O. V. Recent Progress in Surface Hopping: 2011−2015. *J. Phys. Chem. Lett.* **2016**, *7* (11), 2100−2112.
(16) Akimov, A. V.; Neukirch, A. J.; Prezhdo, O. V. Theoretical Insights into Photoinduced Charge Transfer and Catalysis at Oxide Interfaces. *Chem. Rev.* **2013**, *113* (6), 4496−4565.
(17) Wang, Z.; Dong, J.; Wang, L. Large-Scale Surface Hopping Simulation of Charge Transport in Hexagonal Molecular Crystals: Role of Electronic Coupling Signs. *J. Phys.: Condens. Matter* **2023**, *35* (34), No. 345401.
(18) Cheng, K.; Wang, H.; Bang, J.; West, D.; Zhao, J.; Zhang, S. Carrier Dynamics and Transfer across the CdS/MoS 2 Interface upon Optical Excitation. *J. Phys. Chem. Lett.* **2020**, *11* (16), 6544−6550.
(19) Yin, Y.; Zhao, X.; Ren, X.; Liu, K.; Zhao, J.; Zhang, L.; Li, S. Thickness Dependent Ultrafast Charge Transfer in BP/MoS 2 Heterostructure. *Adv. Funct. Mater.* **2022**, *32* (45), No. 2206952.
(20) Borges, I., Jr; Guimarães, R. M. P. O.; Monteiro-de-Castro, G.; Rosa, N. M. P.; Nieman, R.; Lischka, H.; Aquino, A. J. A. A Comprehensive Analysis of Charge Transfer Effects on Donor-Pyrene (Bridge)-Acceptor Systems Using Different Substituents. *J. Comput. Chem.* **2023**, *44* (31), 2424−2436.
(21) Akimov, A. V.; Prezhdo, O. V. Nonadiabatic Dynamics of Charge Transfer and Singlet Fission at the Pentacene/C 60 Interface. *J. Am. Chem. Soc.* **2014**, *136* (4), 1599−1608.
(22) Akimov, A. V. Excited State Dynamics in Monolayer Black Phosphorus Revisited: Accounting for Many-Body Effects. *J. Chem. Phys.* **2021**, *155* (13), No. 134106.
(23) Long, R.; Fang, W.; Akimov, A. V. Nonradiative Electron−Hole Recombination Rate Is Greatly Reduced by Defects in Monolayer Black Phosphorus: Ab Initio Time Domain Study. *J. Phys. Chem. Lett.* **2016**, *7* (4), 653−659.
(24) Zhu, Y.; Long, R.; Fang, W.-H. Substrate Ferroelectric Proximity Effects Have a Strong Influence on Charge Carrier Lifetime in Black Phosphorus. *Nano Lett.* **2023**, *23* (21), 10074−10080.
(25) Ran, J.; Wang, B.; Wu, Y.; Liu, D.; Mora Perez, C.; Vasenko, A. S.; Prezhdo, O. V. Halide Vacancies Create No Charge Traps on Lead Halide Perovskite Surfaces but Can Generate Deep Traps in the Bulk. *J. Phys. Chem. Lett.* **2023**, *14* (26), 6028−6036.
(26) Wang, Y.-F.; Li, Z.-R.; Wu, D.; Sun, C.-C.; Gu, F.-L. Excess electron is trapped in a large single molecular cage C60F60. *J. Comput. Chem.* **2010**, *31* (1), 195−203.
(27) Li, X.; Parrish, R. M.; Martínez, T. J. An Ab Initio Exciton Model for Singlet Fission. *J. Chem. Phys.* **2020**, *153* (18), No. 184116.
(28) Neef, A.; Rossi, M.; Wolf, M.; Ernstorfer, R.; Seiler, H. On the Role of Nuclear Motion in Singlet Exciton Fission: The Case of Single-Crystal Pentacene. *Phys. Status Solidi A* **2024**, *221* (1), No. 2300304.
(29) Lian, M.; Wang, Y.-C.; Peng, S.; Zhao, Y. Photo-Induced Ultrafast Electron Dynamics in Anatase and Rutile TiO_2: Effects of Electron-Phonon Interaction. *Chin. J. Chem. Phys.* **2022**, *35* (2), 270−280.
(30) Jiang, X.; Zheng, Q.; Lan, Z.; Saidi, W. A.; Ren, X.; Zhao, J. Real-Time GW-BSE Investigations on Spin-Valley Exciton Dynamics in Monolayer Transition Metal Dichalcogenide. *Sci. Adv.* **2021**, *7* (10), No. eabf3759.
(31) Zhou, Z.; He, J.; Frauenheim, T.; Prezhdo, O. V.; Wang, J. Control of Hot Carrier Cooling in Lead Halide Perovskites by Point Defects. *J. Am. Chem. Soc.* **2022**, *144* (39), 18126−18134.
(32) Shakiba, M.; Stippell, E.; Li, W.; Akimov, A. V. Nonadiabatic Molecular Dynamics with Extended Density Functional Tight-Binding: Application to Nanocrystals and Periodic Solids. *J. Chem. Theory Comput.* **2022**, *18* (9), 5157−5180.
(33) Shakiba, M.; Akimov, A. V. Dependence of Electron−Hole Recombination Rates on Charge Carrier Concentration: A Case Study of Nonadiabatic Molecular Dynamics in Graphitic Carbon Nitride Monolayers. *J. Phys. Chem. C* **2023**, *127* (19), 9083−9096.
(34) Akimov, A. V. Fundamentals of Trajectory-Based Methods for Nonadiabatic Dynamics. In *Comprehensive Computational Chemistry*; Elsevier, 2024; pp 235−272.
(35) Smith, B.; Akimov, A. V. Modeling Nonadiabatic Dynamics in Condensed Matter Materials: Some Recent Advances and Applications. *J. Phys.: Condens. Matter* **2020**, *32* (7), No. 073001.
(36) Zheng, Q.; Chu, W.; Zhao, C.; Zhang, L.; Guo, H.; Wang, Y.; Jiang, X.; Zhao, J. Ab Initio Nonadiabatic Molecular Dynamics Investigations on the Excited Carriers in Condensed Matter Systems. *WIREs Comput. Mol. Sci.* **2019**, *9* (6), No. e1411.
(37) Blumberger, J. Recent Advances in the Theory and Molecular Simulation of Biological Electron Transfer Reactions. *Chem. Rev.* **2015**, *115* (20), 11191−11238.
(38) Oberhofer, H.; Reuter, K.; Blumberger, J. Charge Transport in Molecular Materials: An Assessment of Computational Methods. *Chem. Rev.* **2017**, *117*, 10319−10357.
(39) Tempelaar, R.; Reichman, D. R. Generalization of Fewest-Switches Surface Hopping for Coherences. *J. Chem. Phys.* **2018**, *148* (10), No. 102309.
(40) Granucci, G.; Persico, M.; Zoccante, A. Including Quantum Decoherence in Surface Hopping. *J. Chem. Phys.* **2010**, *133* (13), No. 134111.
(41) Han, D.; Akimov, A. V. Nonadiabatic Dynamics with Exact Factorization: Implementation and Assessment. *J. Chem. Theory Comput.* **2024**, *20* (12), 5022−5042.
(42) Jaeger, H. M.; Fischer, S.; Prezhdo, O. V. Decoherence-Induced Surface Hopping. *J. Chem. Phys.* **2012**, *137* (22), 22A545.
(43) Jain, A.; Alguire, E.; Subotnik, J. E. An Efficient, Augmented Surface Hopping Algorithm That Includes Decoherence for Use in Large-Scale Simulations. *J. Chem. Theory Comput.* **2016**, *12* (11), 5256−5268.
(44) Shao, C.; Xu, J.; Wang, L. Branching and Phase Corrected Surface Hopping: A Benchmark of Nonadiabatic Dynamics in Multilevel Systems. *J. Chem. Phys.* **2021**, *154* (23), No. 234109.
(45) Sindhu, A.; Jain, A. Benchmarking the Surface Hopping Method to Include Nuclear Quantum Effects. *J. Chem. Theory Comput.* **2021**, *17* (2), 655−665.
(46) Dutra, M.; Wickramasinghe, S.; Garashchuk, S. Quantum Dynamics with the Quantum Trajectory-Guided Adaptable Gaussian Bases. *J. Chem. Theory Comput.* **2020**, *16* (1), 18−34.
(47) Dutra, M.; Garashchuk, S.; Akimov, A. V. The Quantum Trajectory-Guided Adaptive Gaussian Methodology in the Libra Software Package. *Int. J. Quantum Chem.* **2023**, *123* (8), No. e27078.
(48) Donoso, A.; Martens, C. C. Quantum Tunneling Using Entangled Classical Trajectories. *Phys. Rev. Lett.* **2001**, *87* (22), No. 223202.
(49) Dupuy, L.; Talotta, F.; Agostini, F.; Lauvergnat, D.; Poirier, B.; Scribano, Y. Adiabatic and Nonadiabatic Dynamics with Interacting Quantum Trajectories. *J. Chem. Theory Comput.* **2022**, *18* (11), 6447−6462.
(50) Jain, A.; Sindhu, A. Pedagogical Overview of the Fewest Switches Surface Hopping Method. *ACS Omega* **2022**, *7* (50), 45810−45824.
(51) Akimov, A. V. A Simple Phase Correction Makes a Big Difference in Nonadiabatic Molecular Dynamics. *J. Phys. Chem. Lett.* **2018**, *9* (20), 6096−6102.
(52) Zhou, Z.; Jin, Z.; Qiu, T.; Rappe, A. M.; Subotnik, J. E. A Robust and Unified Solution for Choosing the Phases of Adiabatic States as a Function of Geometry: Extending Parallel Transport Concepts to the Cases of Trivial and Near-Trivial Crossings. *J. Chem. Theory Comput.* **2020**, *16* (2), 835−846.
(53) Meek, G. A.; Levine, B. G. Evaluation of the Time-Derivative Coupling for Accurate Electronic State Transition Probabilities from Numerical Simulations. *J. Phys. Chem. Lett.* **2014**, *5* (13), 2351−2356.
(54) Temen, S.; Akimov, A. V. A Simple Solution to Trivial Crossings: A Stochastic State Tracking Approach. *J. Phys. Chem. Lett.* **2021**, *12* (2), 850−860.
(55) Bai, X.; Qiu, J.; Wang, L. An Efficient Solution to the Decoherence Enhanced Trivial Crossing Problem in Surface Hopping. *J. Chem. Phys.* **2018**, *148* (10), No. 104106.

https://doi.org/10.1021/acs.jpclett.4c02909
J. Phys. Chem. Lett. 2024, 15, 11944−11953

(56) Fernandez-Alberti, S.; Roitberg, A. E.; Nelson, T.; Tretiak, S. Identification of Unavoided Crossings in Nonadiabatic Photoexcited Dynamics Involving Multiple Electronic States in Polyatomic Conjugated Molecules. *J. Chem. Phys.* **2012**, *137* (1), No. 014512.
(57) Carof, A.; Giannini, S.; Blumberger, J. Detailed Balance, Internal Consistency, and Energy Conservation in Fragment Orbital-Based Surface Hopping. *J. Chem. Phys.* **2017**, *147* (21), No. 214113.
(58) Wang, L.; Prezhdo, O. V. A Simple Solution to the Trivial Crossing Problem in Surface Hopping. *J. Phys. Chem. Lett.* **2014**, *5* (4), 713−719.
(59) Fernandez-Alberti, S.; Roitberg, A. E.; Nelson, T.; Tretiak, S. Identification of Unavoided Crossings in Nonadiabatic Photoexcited Dynamics Involving Multiple Electronic States in Polyatomic Conjugated Molecules. *J. Chem. Phys.* **2012**, *137* (1), No. 014512.
(60) Ryabinkin, I. G.; Nagesh, J.; Izmaylov, A. F. Fast Numerical Evaluation of Time-Derivative Nonadiabatic Couplings for Mixed Quantum−Classical Methods. *J. Phys. Chem. Lett.* **2015**, *6* (21), 4200−4203.
(61) Giannini, S.; Carof, A.; Blumberger, J. Crossover from Hopping to Band-Like Charge Transport in an Organic Semiconductor Model: Atomistic Nonadiabatic Molecular Dynamics Simulation. *J. Phys. Chem. Lett.* **2018**, *9* (11), 3116−3123.
(62) Akimov, A. V.; Prezhdo, O. V. The PYXAID Program for Non-Adiabatic Molecular Dynamics in Condensed Matter Systems. *J. Chem. Theory Comput.* **2013**, *9* (11), 4959−4972.
(63) Shih, B.-C.; Xue, Y.; Zhang, P.; Cohen, M. L.; Louie, S. G. Quasiparticle Band Gap of ZnO: High Accuracy from the Conventional G 0 W 0 Approach. *Phys. Rev. Lett.* **2010**, *105* (14), No. 146401.
(64) Zhang, Y.; Xia, W.; Wu, Y.; Zhang, P. Prediction of MXene Based 2D Tunable Band Gap Semiconductors: GW Quasiparticle Calculations. *Nanoscale* **2019**, *11* (9), 3993−4000.
(65) van Setten, M. J.; Caruso, F.; Sharifzadeh, S.; Ren, X.; Scheffler, M.; Liu, F.; Lischner, J.; Lin, L.; Deslippe, J. R.; Louie, S. G.; Yang, C.; Weigend, F.; Neaton, J. B.; Evers, F.; Rinke, P. GW100: Benchmarking G0W0 for Molecular Systems. *J. Chem. Theory Comput.* **2015**, *11* (12), 5665−5687.
(66) Kühne, T. D.; Iannuzzi, M.; Del Ben, M.; Rybkin, V. V.; Seewald, P.; Stein, F.; Laino, T.; Khaliullin, R. Z.; Schütt, O.; Schiffmann, F.; Golze, D.; Wilhelm, J.; Chulkov, S.; Bani-Hashemian, M. H.; Weber, V.; Borštnik, U.; Taillefumier, M.; Jakobovits, A. S.; Lazzaro, A.; Pabst, H.; Müller, T.; Schade, R.; Guidon, M.; Andermatt, S.; Holmberg, N.; Schenter, G. K.; Hehn, A.; Bussy, A.; Belleflamme, F.; Tabacchi, G.; Glöß, A.; Lass, M.; Bethune, I.; Mundy, C. J.; Plessl, C.; Watkins, M.; VandeVondele, J.; Krack, M.; Hutter, J. CP2K: An Electronic Structure and Molecular Dynamics Software Package - Quickstep: Efficient and Accurate Electronic Structure Calculations. *J. Chem. Phys.* **2020**, *152* (19), No. 194103.
(67) Furche, F.; Ahlrichs, R. Adiabatic Time-Dependent Density Functional Methods for Excited State Properties. *J. Chem. Phys.* **2002**, *117* (16), 7433−7447.
(68) Fdez. Galván, I.; Vacher, M.; Alavi, A.; Angeli, C.; Aquilante, F.; Autschbach, J.; Bao, J. J.; Bokarev, S. I.; Bogdanov, N. A.; Carlson, R. K.; Chibotaru, L. F.; Creutzberg, J.; Dattani, N.; Delcey, M. G.; Dong, S. S.; Dreuw, A.; Freitag, L.; Frutos, L. M.; Gagliardi, L.; Gendron, F.; Giussani, A.; González, L.; Grell, G.; Guo, M.; Hoyer, C. E.; Johansson, M.; Keller, S.; Knecht, S.; Kovačević, G.; Källman, E.; Li Manni, G.; Lundberg, M.; Ma, Y.; Mai, S.; Malhado, J. P.; Malmqvist, P. Å.; Marquetand, P.; Mewes, S. A.; Norell, J.; Olivucci, M.; Oppel, M.; Phung, Q. M.; Pierloot, K.; Plasser, F.; Reiher, M.; Sand, A. M.; Schapiro, I.; Sharma, P.; Stein, C. J.; Sørensen, L. K.; Truhlar, D. G.; Ugandi, M.; Ungur, L.; Valentini, A.; Vancoillie, S.; Veryazov, V.; Weser, O.; Wesołowski, T. A.; Widmark, P.-O.; Wouters, S.; Zech, A.; Zobel, J. P.; Lindh, R. OpenMolcas: From Source Code to Insight. *J. Chem. Theory Comput.* **2019**, *15* (11), 5925−5964.
(69) Belyaev, A. K.; Lebedev, O. V. Nonadiabatic Nuclear Dynamics of Atomic Collisions Based on Branching Classical Trajectories. *Phys. Rev. A* **2011**, *84* (1), No. 014701.
(70) T. do Casal, M.; Toldo, J. M.; Pinheiro, M., Jr; Barbatti, M. Fewest Switches Surface Hopping with Baeck-An Couplings. *Open Research Europe* **2021**, *1*, 49.
(71) Baeck, K. K.; An, H. Practical Approximation of the Non-Adiabatic Coupling Terms for Same-Symmetry Interstate Crossings by Using Adiabatic Potential Energies Only. *J. Chem. Phys.* **2017**, *146* (6), No. 064107.
(72) Iwasa, N.; Nanbu, S. Investigating the Photo-Relaxation Mechanism of 6-Azauracil through Ab Initio Nonadiabatic Molecular Dynamics Simulations. *Chem. Phys. Lett.* **2024**, *838*, No. 141088.
(73) Yu, L.; Xu, C.; Lei, Y.; Zhu, C.; Wen, Z. Trajectory-Based Nonadiabatic Molecular Dynamics without Calculating Nonadiabatic Coupling in the Avoided Crossing Case: Trans ↔ Cis Photoisomerization in Azobenzene. *Phys. Chem. Chem. Phys.* **2014**, *16* (47), 25883−25895.
(74) Hanasaki, K.; Kanno, M.; Niehaus, T. A.; Kono, H. An Efficient Approximate Algorithm for Nonadiabatic Molecular Dynamics. *J. Chem. Phys.* **2018**, *149* (24), No. 244117.
(75) Akimov, A. V. The Fewest Switches Surface Hopping as an Optimisation Problem. *Mol. Phys.* **2024**, *0* (0), No. e2376893.
(76) Wang, L.; Trivedi, D.; Prezhdo, O. V. Global Flux Surface Hopping Approach for Mixed Quantum-Classical Dynamics. *J. Chem. Theory Comput.* **2014**, *10* (9), 3598−3605.
(77) Jasper, A. W.; Truhlar, D. G. Improved Treatment of Momentum at Classically Forbidden Electronic Transitions in Trajectory Surface Hopping Calculations. *Chem. Phys. Lett.* **2003**, *369* (1−2), 60−67.
(78) Shakiba, M.; Akimov, A. V. Generalization of the Local Diabatization Approach for Propagating Electronic Degrees of Freedom in Nonadiabatic Dynamics. *Theor. Chem. Acc.* **2023**, *142* (8), 68.
(79) Granucci, G.; Persico, M.; Toniolo, A. Direct Semiclassical Simulation of Photochemical Processes with Semiempirical Wave Functions. *J. Chem. Phys.* **2001**, *114* (24), 10608−10615.
(80) Shakiba, M.; Akimov, A. V. Machine-Learned Kohn−Sham Hamiltonian Mapping for Nonadiabatic Molecular Dynamics. *J. Chem. Theory Comput.* **2024**, *20* (8), 2992−3007.
(81) Hammes-Schiffer, S.; Tully, J. C. Nonadiabatic Transition State Theory and Multiple Potential Energy Surface Molecular Dynamics of Infrequent Events. *J. Chem. Phys.* **1995**, *103* (19), 8528−8537.
(82) Esch, M. P.; Levine, B. G. Decoherence-Corrected Ehrenfest Molecular Dynamics on Many Electronic States. *J. Chem. Phys.* **2020**, *153* (11), No. 114104.
(83) Akimov, A. V. Libra: An Open-Source "Methodology Discovery" Library for Quantum and Classical Dynamics Simulations. *J. Comput. Chem.* **2016**, *37* (17), 1626−1649.
(84) Shakiba, M.; Smith, B.; Li, W.; Dutra, M.; Jain, A.; Sun, X.; Garashchuk, S.; Akimov, A. Libra: A Modular Software Library for Quantum Nonadiabatic Dynamics. *Softw. Impacts* **2022**, *14*, No. 100445.
(85) Akimov, A. V.; Shakiba, M.; Smith, B.; Han, D.; Dutra, M.; Sato, K.; Gerasimov, I. S.; Temen, S.; Li, W.; Khvorost, T.; Sun, X.; Stippell, L.; Qingxin, Z. *Quantum-Dynamics-Hub/Libra-Code: Libra*, ver. 5.8.1; 2024 DOI: 10.5281/zenodo.14043087 (accessed 2024-11-05).
(86) Akimov, A. V. *Project_F_tracking*, ver. 1.2.0; 2024 (accessed 2024-11-05).

https://doi.org/10.1021/acs.jpclett.4c02909
J. Phys. Chem. Lett. 2024, 15, 11944−11953